

Kinetic Model Evaluation of Dynamical Properties of Nanoantennas Embedded in a Polymer Carrying the Nuclei of Fusion Fuel

István Papp^{1,2}, Larissa Bravina⁴, Mária Csete^{1,5}, Archana Kumari^{1,2}, Igor N. Mishustin⁶,
Anton Motornenko⁶, Péter Rácz^{1,2}, Leonid M. Satarov⁶, Horst Stöcker^{6,7,8}, Daniel D. Strottman⁹,
András Szenes^{1,5}, Dávid Vass^{1,5}, Ágnes Nagyné Szokol^{1,2}, Judit Kámán^{1,2}, Attila Bonyár¹⁰,
Tamás S. Biró^{1,2}, László P. Csernai^{1,2,3,6,11}, Norbert Kroó^{1,2,12}
(part of NAPLIFE Collaboration)

¹ Wigner Research Centre for Physics, Budapest, Hungary

² Hungarian Bureau for Research Development and Innovation

³ Dept. of Physics and Technology, University of Bergen, Norway

⁴ Department of Physics, University of Oslo, Norway

⁵ Dept. of Optics and Quantum Electronics, Univ. of Szeged, Hungary

⁶ Frankfurt Institute for Advanced Studies, Frankfurt/Main, Germany

⁷ Inst. für Theoretische Physik, Goethe Universität, Frankfurt/Main, Germany

⁸ GSI Helmholtzzentrum für Schwerionenforschung GmbH, Darmstadt, Germany

⁹ Los Alamos National Laboratory, Los Alamos, New Mexico, USA

¹⁰ Department of Electronics Technology, Faculty of Electrical Engineering and Informatics
Budapest University of Technology and Economics, Hungary

¹¹ Csernai Consult Bergen, Bergen, Norway

¹² Hungarian Academy of Sciences, Budapest, Hungary

Abstract

Recently laser induced fusion with simultaneous volume ignition, a spin-off from relativistic heavy ion collisions, was proposed, where implanted nanoantennas regulated and amplified the light absorption in the fusion target. Studies of resilience of the nanoantennas was published recently in vacuum. These studies are extended to nanoantennas embedded into a polymer, which modifies the nanoantenna's lifetime and absorption properties.

Keywords: particle-in-cell method, gold nanoparticles, plasmonic effect, polymer

1. Introduction

NANOPlasmonic Laser Inertial Fusion Experiments (NAPLIFE) [1] is an improved way to achieve laser driven fusion in a non-thermal, collider configuration to avoid instabilities during ignition. It is based on simultaneous (or "time-like") ignition [2, 3], with enhanced energy absorption with the help of nanoantennas implanted into the target material [4]. This should prevent the development of the mechanical Rayleigh-Taylor instability. Furthermore, the nuclear burning should not propagate from a central hot spot to the outside edge as the ignition is simultaneous in the whole volume.

Non-equilibrium and linear colliding configuration have been introduced already [5, 6]. Here we study the idea of layered flat target fuel with embedded nanorod antennas, that regulate laser light absorption to enforce simultaneous ignition. We plan a seven-layer flat target with different nanorod densities. [7, 8, 9]. In order to prepare such a layered target, the ignition fuel (e.g. deuterium, D, tritium, T, or other nuclei for fusion) are embedded into a hard thin polymer material of seven, 3 μm thick layers. These polymers are Urethane Dimethacrylate (UDMA) and Triethylene glycol dimethacrylate (TEGDMA) in (3:1) mass ratio [10, 11]. The UDMA polymer molecule con-

tains 470 nuclei, 38 of them are Hydrogen. One can also use deuterized UDMA, where some of the Hydrogens are replaced by Deuterium atoms.

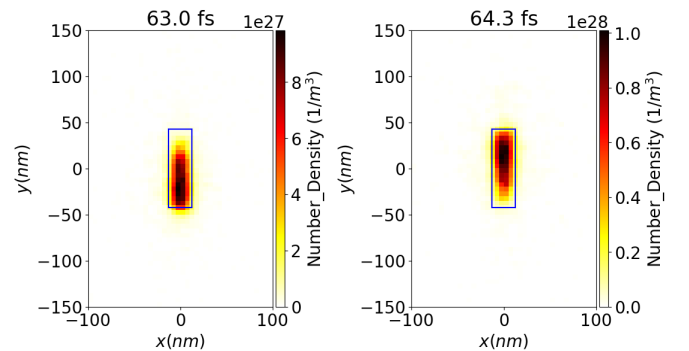


Figure 1: (color online) Cross section of the 25 nm (diameter) x 85 nm nanorod showing Number density of electrons at the tips at different times t , half of the light wave time period apart, show electrons leaving the nanorod. The number of electron marker-particles inside the simulation box will decrease with a significant amount by the end of simulation at 120 fs.

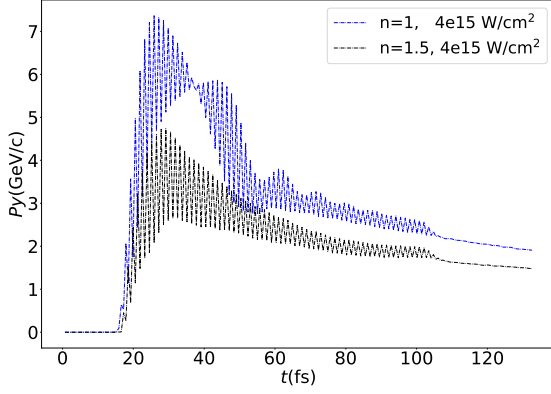


Figure 2: (color online) We consider a laser pulse of intensity $I = 4 \cdot 10^{15} \text{ W/cm}^2$ and duration of 106fs. Here we show the time dependence of the total y directed momentum of the conducting electrons in the nanorod. The nanorod is in surrounding UDMA polymer (black line) and in vacuum (blue line). The UDMA polymer decreases the momentum of the emitted electrons considerably compared to the emission to vacuum. An interesting “beat” interference is occurring in case of emission to vacuum. Apparently the nanorod antenna in vacuum has two slightly different resonant frequencies. The rate of beat is $\sim 5 \cdot 10^{13} \text{ Hz}$, while the frequency of the driving laser beam is $3.8 \cdot 10^{14} \text{ Hz}$ ($T = 2.65 \text{ fs}$). In UDMA the beating does not occur as the somewhat random surface between the gold nanorod and the kinetic model representation of UDMA does not lead to two distinct resonance frequencies.

2. Dynamics of the resonance in the nanorod

When a resonant nanoparticle of a size related to the effective wavelength of light a localised surface plasmon (LSP) is created. When the coherently oscillating electric field irradiates the metallic nanoparticle it causes the conduction electrons to oscillate also. The Coulomb attraction between electrons and nuclei produces a restoring force when the electron cloud is moved from its initial location. The electron cloud oscillates due to this force. The effective electron mass, the size and form of the charge distribution, and the electron density all contribute to the oscillation frequency. The LSP has two key effects: it dramatically increases electric fields near the nanoparticle’s surface and it increases optical absorption at the plasmon resonance frequency. The form of the nanoparticle can also be used to adjust surface plasmon resonance [12, 13].

A recent kinetic theoretical study analyzed the resilience of nanorod antennas under a short laser pulse irradiation in vacuum [14].

Now we extend these studies to nanorod antennas embedded into the UDMA polymer. Here we consider the refracting index of UDMA ($n=1.53$) [11], which slows down the propagation of light. The short laser pulse is chosen to have a length needed to propagate across the target of $7 \cdot 3\mu\text{m} = 21\mu\text{m}$ thickness. The nanorods are orthogonal to the direction of laser irradiation in this model study.

The conduction electrons show behavior of strongly coupled plasma [15]. The gold antennas are smaller than the half wavelength of the irradiated light. At optical frequencies the classical ideal half-wavelength dipole antenna scaling of rod with length $L = \lambda/2$ breaks down. Here instead an effective wavelength needs to be considered [15]. When the nanorods are embedded in a surrounding medium different from vacuum the

effective wavelength scales as follows:

$$\frac{\lambda_{eff}}{2R\pi} = 13.74 - 0.12[\varepsilon_{\infty} + \varepsilon_s 141.04]/\varepsilon_s - \frac{2}{\pi} + \frac{\lambda}{\lambda_p} 0.12 \sqrt{\varepsilon_{\infty} + \varepsilon_s 141.04}/\varepsilon_s \quad (1)$$

where $\varepsilon_{\infty} = 11$ is the dielectric function in the infinite frequency limit [16] and $\lambda_p = 138 \text{ nm}$ is the plasma wavelength for gold. The propagation velocity of light inside the medium is reduced to $c_s = 1/\sqrt{\varepsilon_s}$, therefore $\varepsilon_s = n^2$. This is a good motivation for using Particle in Cell (PIC) methods for studying this behavior. We used similar principles as described in [14], using the EPOCH computing package [17, 18, 19]. We considered nanorod antennas with partly ionised gold atoms with three conducting electrons per gold atoms.

Initially electrons in the $\lambda_{eff}/2 = 85 \text{ nm}$ [8] nanorod antenna follow the phase of the laser irradiation with $t = 2.65 \text{ fs}$ period. With time electrons diffuse out of the nanorod, mainly at its two ends (Fig. 1). The potential wall to UDMA keeping the electrons in the nanorod is apparently smaller than in the case of surrounding vacuum [14].

Simulation studies using the COMSOL Multiphysics Finite Element Method (FEM) package with many parameters found absorptivities between 0.085 and 0.192 for nanorod antennas [7]. By varying the density of implanted nanoantennas one could achieve almost uniform integrated energy absorption at a given overlapping time of 240 fs for two counter-propagating 120 fs laser pulses [7, 20].

The beam intensity utilized was $I = 4 \cdot 10^{15} \text{ W/cm}^2$ so that the plasmonic nanoantennas are not destroyed before the laser pulse passes. This damage threshold also depends on the geometry and size of the nanoantennas.

We compared the time dependence of momentum of escaping electrons in vacuum and in UDMA. The magnitude and the dynamics of electron emission is quite different, as shown in Fig. 2.

The gold nanorods may lose a few electrons from the conduction band without destroying their solid structure, so they still can enhance the absorptivity of the ignition pulse for about 20-50 fs, leaving enough time for the full ignition.

For the emission of a single electron from gold plasmonic nanoantennas four 795 nm photons are needed. On the other hand the incoming pulse generates a surface plasmon, which may later emit electrons. This indirect process is more frequent than the direct emission by four photons [21, 22].

Similarly to the analysis in ref. [14] we now study the energy transfer dynamics from the laser irradiation to the target, with and without nanorods.

Consider now an intense laser beam ($\lambda = 795 \text{ nm}$ in vacuum and $795/1.53$ in UDMA), with intensity $I = 4 \cdot 10^{15} \text{ W/cm}^2$, irradiating a calculation box (CB) of cross section $S_{CB} = 530 \cdot 530 \text{ nm}^2 = 2.81 \cdot 10^{-9} \text{ cm}^2$ and of length $L_{CB} = \lambda = 795 \text{ nm}$, with a step-function time profile of pulse length $T_P = 106 \text{ fs}$ ($\sim 40\lambda/c$). The laser pulse energy fraction falling into this box is $E_P = 1.19 \mu\text{J}$. In the geometrical middle we insert a single nanorod antenna of length 85 nm and diameter 25 nm. As the

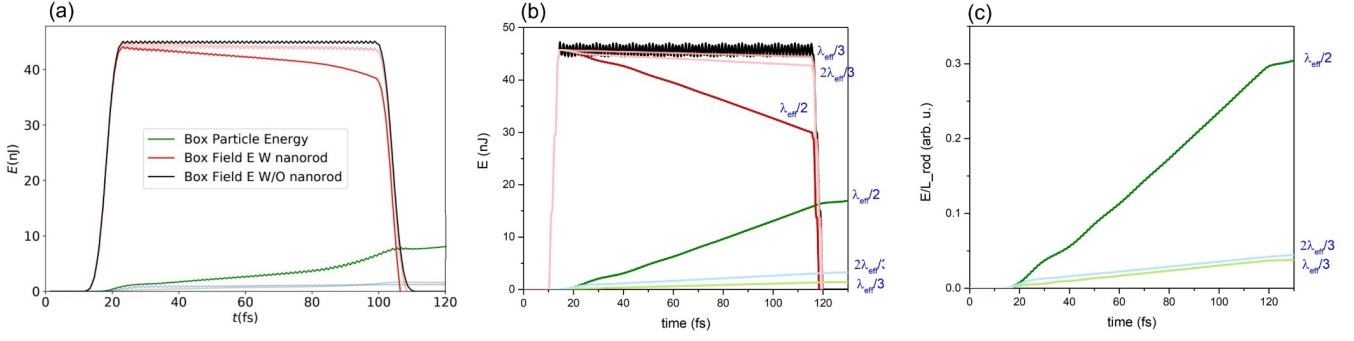


Figure 3: (color online) Optical response of the gold nanorod with different numerical methods and lengths, $L = \lambda_{eff}/2$, $\lambda_{eff}/3$ and $2\lambda_{eff}/3$, (a) PIC, (b) FEM and (c) FEM with normalized values to unit antenna length. The tendencies of the time-evolution of the nanorod energy determined by PIC and FEM are in very good agreement. The energy in the calculation box increases rapidly till about 20 fs, then it becomes constant (without nanoantenna) until the laser pulse lasts, at this moment the energy in the box drops to zero. With the nanoantenna in the box the resonant antenna absorbs a good part of the laser energy, (green line), while much less for the non resonant length antennas. There is a quantitative difference between the rates of energy increase, namely the slope is significantly smaller for PIC computations, accordingly the value achieved at 106 fs is also smaller. The smaller slope is caused by the tunneling of the electrons out of the antenna that is included into the PIC computations but not in FEM. The (c) figure shows that the difference between the two non-resonant antennas is caused by the antenna lengths, when this is removed by the length normalization the difference vanishes.

calculation box size (λ) is $1.53 \cdot 1/40$ th of the irradiation pulse length (40λ), the initial and final transients are negligible. See Fig. 3.

We used two different marker particle species, 42500 positively charged gold ions (+3) and three (127500) conducting electrons for each, being careful to the neutral charge of the nanoantenna. We define the size of the nanorod, indicating the limits where the particle number density becomes zero. The borders of which can be seen in Fig. 1.

We consider three situations, the box contains (i) vacuum, (ii) UDMA polymer and (iii) UDMA polymer with gold nanorod antenna in the middle of the box.

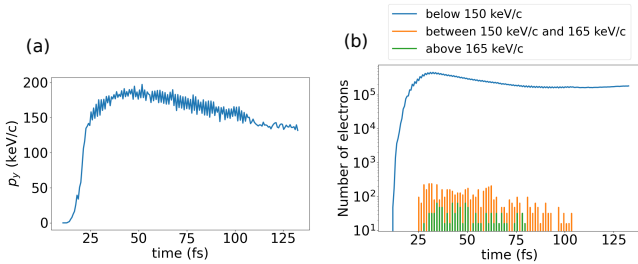


Figure 4: (color online) The behaviour of electrons leaving the nanorod. Flat plateau laser light reaches the nanorod with maximum intensity at around 20 fs and leaves the calculation box at 106 fs. Figure (a) indicates the maximum momentum in time reached by a spilled out electron in the y direction. Figure (b) shows the distribution of electrons at different y direction momentum values. Below 150 keV/c (blue line), above 150 keV/c (orange line) and above 165 keV/c (green line).

We consider the following processes for direct absorption to the UDMA. As UDMA is transparent the light absorption is minimal, while the refractive index is $n = 1.53$. The absorption coefficient of the bare polymer matrix at this wavelength would be $\approx 0.3 \text{ cm}^{-1}$ while doped with gold nanorods it would reach 18 cm^{-1} [11].

In the EPOCH PIC kinetic plasma simulations model one is

usually interested in charged particles, where the surrounding medium is vacuum. However, here we simulate metal nanoantenna with conducting electrons approached as plasma and the UDMA polymer is taken into account with a relative electric permittivity different from vacuum. The wavelength inside the simulation box containing UDMA is also shrunk according to the refractive index.

3. Conclusions and Outlook

The result of this simulation shows that the resilience of the nanoantenna in the UDMA polymer is similar to the vacuum case. In case of vacuum at 19 fs, when the maximum intensity of the laser reaches the nanorod, most electrons, $N_e = 10^3$, have 0.015 MeV/c momentum in the y direction. However at the time when the irradiation finishes at 106 fs, around $N_e = 2 \times 10^2$ electrons remain at this momentum [14]. Other electrons escape at the tip of the nanorod. At 43 fs the the number of leaving electrons reach the maximum while also achieving the maximum momentum in the y direction (Fig. 4). Potential difference becomes $E_y = +/ - 2.9 \times 10^{12} \text{ V/m} = +/ - 2.9 \times 10^3 \text{ V/nm}$. Maximum momentum of leaving electrons in the y direction reaches 0.3025 MeV/c in vacuum, in UDMA at the same time the maximum is lower at 0.1799 MeV/c . The total momentum amplitude at this time is also lower in 4.5 GeV/c in UDMA compared to 7.5 GeV/c in vacuum.

The decay time of the nanoantenna is somewhat shorter but sufficient for the initial volume ignition. The absorbed energy from the CB to the nanoantenna and the polymer is slightly less, but this is understandable as the single nanoantenna's length now is only 85 nm while in the case of vacuum it was 130 nm.

With this extended study we see that in the case of vacuum the time dependence of the momentum absorption shows a beat pattern due to two nearly identical resonance frequencies. Inside UDMA this beating is not present and the absorption is less as it is shown in Fig. 2 also.

Similar to [14] we also studied the time dependence of the momentum fluctuation of the electrons. Now the proton fluctuations were also studied. Initially the proton distribution slightly lags behind the electrons indicating that the electrons are pulling the protons. At later time as the laser drive is over the two distributions become aligned in phase. This phenomena will need further investigation.

The time dependence of the energy absorption by a nanorod in UDMA polymer was also studied in the COMSOL Multiphysics model. The results are similar, the main difference between the two models is arising from the different treatment of the conducting electrons. In the PIC model the conduction band electrons move freely and can escape leaving the gold ions behind, in the traditional, FEM approach the electrons' collective motion is taken into account indirectly through damping constants and they cannot leave from the surface of the nanorod.

4. Acknowledgements

Enlightening discussions with Johann Rafelski are gratefully acknowledged. Horst Stöcker acknowledges the Judah M. Eisenberg Professor Laureatus chair at Fachbereich Physik of Goethe Universität Frankfurt. We would like to thank the Wigner GPU Laboratory at the Wigner Research Center for Physics for providing support in computational resources. This work is supported in part by the Frankfurt Institute for Advanced Studies, Germany, the Eötvös Loránd Research Network of Hungary, the Research Council of Norway, grant no. 255253, and the National Research, Development and Innovation Office of Hungary, via the projects: Nanoplasmonic Laser Inertial Fusion Research Laboratory (NKFIH-468-3/2021), Optimized nanoplasmonics (K116362), and Ultrafast physical processes in atoms, molecules, nanostructures and biological systems (EFOP-3.6.2-16-2017-00005). L.P. Csernai acknowledges support from Wigner RCP, Budapest (2022-2.2.1-NL-2022-00002)

References

- [1] L.P. Csernai, M. Csete, I.N. Mishustin, A. Motornenko, I. Papp, L.M. Satarov, H. Stöcker & N. Kroó, Radiation-Dominated Implosion with Flat Target, *Physics and Wave Phenomena*, **28** (3) 187-199 (2020). (arXiv:1903.10896v3).
- [2] L.P. Csernai, Detonation on Timelike Front for Relativistic Systems, School of Physics, University of Minnesota, Minneapolis, Minnesota, USA, *Zh. Eksp. Teor. Fiz.* **92**, 397-386 (1987), & *Sov. Phys. JETP* **65**, 219 (1987).
- [3] L.P. Csernai, & D.D. Strottman, Volume Ignition via Time-Like Detonation in Pellet Fusion, *Laser and Particle Beams* **33**, 279-282 (2015).
- [4] L.P. Csernai, N. Kroó, & I. Papp, Radiation-Dominated Implosion with Nano-Plasmonics, *Laser and Particle Beams* **36**, 171-178 (2018).
- [5] M. Barbarino, Fusion reactions in laser produced plasma, PhD thesis, Texas A&M University (2015).
- [6] G. Zhang, M. Huang, A. Bonasera, Y. G. Ma, B. F. Shen, H. W. Wang, J. C. Xu, G. T. Fan, H. J. Fu, H. Xue, H. Zheng, L. X. Liu, S. Zhang, W. J. Li, X. G. Cao, X. G. Deng, X. Y. Li, Y. C. Liu, Y. Yu, Y. Zhang, C. B. Fu, and X. P. Zhang, Nuclear probes of an out-of-equilibrium plasma at the highest compression, *Phys. Lett. A* **383** (19), 2285-2289 (2019).
- [7] M. Csete, A. Szenes, E. Tóth, D. Vass, O. Fekete, B. Bánhelyi, I. Papp, T. S. Biró, L. P. Csernai, N. Kroó (NAPLIFE Collaboration), Comparative study on the uniform energy deposition achievable via optimized plasmonic nanoresonator distributions, *Plasmonics* **17** (2), 775-787 (2022). <https://doi.org/10.1007/s11468-021-01571-x>. (2022)
- [8] A. Bonyár et al., (NAPLIFE Collaboration), Nanoplasmonic Laser Fusion Target Fabrication - Considerations and Preliminary Results, Int. Conf. on New Frontiers in Physics, Kolymbari, Crete, Greece, Sept. 11, 2020.
- [9] M. Csete, et al. Plasmonic nanoresonator distributions for uniform energy deposition in active targets, *Optical Materials Express* (2022), accepted for publication
- [10] Izabela M. Barszczewska-Rybarek Structure-property relationships in dimethacrylate networks based on Bis-GMA, UDMA and TEGDMA, *Dental Materials*, Volume **25**, Issue 9, 2009, Pages 1082-1089
- [11] Bonyár A, Szalóki M, Borók A, Rigó I, Kámán J, Zangana S, Veres M, Rácz P, Aladi M, Kedves MÁ, Szokol Á, Petrik P, Fogarassy Z, Molnár K, Csete M, Szenes A, Tóth E, Vas D, Papp I, Galbács G, Csernai LP, Biró TS, Kroó N, Collaboration N. The Effect of Femtosecond Laser Irradiation and Plasmon Field on the Degree of Conversion of a UDMA-TEGDMA Copolymer Nanocomposite Doped with Gold Nanorods. *International Journal of Molecular Sciences*. 2022; 23(21):13575
- [12] K. Lance Kelly, Eduardo Coronado, Lin Lin Zhao, and George C. Schatz The Journal of Physical Chemistry B 2003 107 (3), 668-677
- [13] S. A. Maier, Plasmonics: Fundamentals and Applications, New York, NY, Springer Science & Business Media (2007).
- [14] István Papp, Larissa Bravina, Mária Csete, Archana Kumari, Igor N. Mishustin, Dénes Molnár, Anton Motornenko, Péter Rácz, Leonid M. Satarov, Horst Stöcker, Daniel D. Strottman, András Szenes, Dávid Vass, Tamás S. Biró, László P. Csernai, and Norbert Kroó, (NAPLIFE Collaboration), Kinetic Model Evaluation of the Resilience of Plasmonic Nanoantennas for Laser-Induced Fusion, *PRX Energy*, **1**, 023001 (2022).
- [15] Lukas Novotny, Effective Wavelength Scaling for Optical Antennas, *Phys. Rev. Lett.* **98**, 266802 (2007).
- [16] M. S. Dresselhaus, Solid State Physics - Part II Optical Properties of Solids, (MIT Lecture Notes, 2001)
- [17] T. D. Arber, et. al. Contemporary particle-in-cell approach to laser-plasma modelling, *Plasma Phys. Control. Fusion* **57**, 113001 (2015)
- [18] K. Nanbu, S. Yonemura. Weighted particles in coulomb collision simulations based on the theory of a cumulative scattering angle. *Journal of Computational Physics*, vol. **145**, pp. 639-654 (1998).
- [19] F. Pérez, L. Gremillet, A. Decoster, M. Drouin, E. Lefebvre. Improved modeling of relativistic collisions and collisional ionization in particle-in-cell codes. *Physics of Plasmas*, vol. **19**, no. 8, Aug. (2012).
- [20] István Papp, Larissa Bravina, Mária Csete, Igor N. Mishustin, Dénes Molnár, Anton Motornenko, Leonid M. Satarov, Horst Stöcker, Daniel D. Strottman, András Szenes, Dávid Vass, Tamás S. Biró, László P. Csernai, Norbert Kroó, (NAPLIFE Collaboration) Laser Wake Field Collider; *Phys. Lett. A* **396**, 12724 (2021).
- [21] M. Merschdorf, W. Pfeiffer, A. Thon, S. Voll, G. Gerber, Photoemission from multiply excited surface plasmons in Ag nanoparticles, *Appl. Phys. A* **71**, 547-552 (2000).
- [22] Gy. Farkas, Z.Gy. Horváth, Multiphoton electron emission processes induced by different kinds of ultrashort laser pulses, *Optics Comm.* **12** (1974) 392-395; Gy. Farkas, Z. Gy. Horváth, and Cs. Tóth Linear surface photoelectric effect of gold in intense laser field as a possible high-current electron source, *J. of Appl. Phys.* **62** (1987) 4545.